

# Spin-polarized currents through interacting quantum wires with nonmagnetic leads

J.E. Birkholz<sup>1</sup> and V. Meden<sup>2</sup>

<sup>1</sup>*Institut für Theoretische Physik, Universität Göttingen,  
Friedrich-Hund-Platz 1, D-37077 Göttingen, Germany*

<sup>2</sup>*Institut für Theoretische Physik A, RWTH Aachen University and  
JARA—Fundamentals of Future Information Technology, D-52056 Aachen, Germany*

We study the performance of a quantum wire spin filter that is based on the Rashba spin-orbit interaction in the presence of the electron-electron interaction. The finite length wire is attached to two semi-infinite nonmagnetic leads. Analyzing the spin polarization of the linear conductance at zero temperature, we show that spin-filtering is possible by adequate tuning of the system parameters first considering noninteracting electrons. Next, the functional renormalization group method is used to capture correlation effects induced by the Coulomb interaction. For short wires we show that the energy regime in which spin polarization is found is strongly affected by the Coulomb interaction. For long wires we find the power-law suppression of the total conductance on low energy scales typical for inhomogeneous Luttinger liquids while the degree of spin polarization stays constant.

PACS numbers: 72.25.Dc, 71.70.Ej, 72.25.Mk, 71.10.Pm

## I. INTRODUCTION

The birth of *spintronics* can be dated back to the discovery of the *giant magnetoresistance* effect in 1988.<sup>1,2</sup> Since then, many theoretical and experimental studies on spin-dependent electronic transport have been performed in order to achieve a clear understanding of the underlying physics and to investigate the possibility of fabricating spintronic devices.<sup>3,4,5</sup> One manifest realization of such a device is a quantum wire with parameters which can be tuned by a set of gate electrodes such that the transport of electrons with a certain spin direction is favored. The original proposal by Datta and Das<sup>3</sup> is to use the spin precession in a narrow-gap semiconductor wire with spin-orbit coupling between two magnetized leads to modulate the current. However, Strēda and Sēba came up with an idea of obtaining spin polarization in a (almost) nonmagnetic system. They considered transport through an *infinite* quasi one-dimensional (1D) quantum wire with Rashba spin-orbit interaction (SOI), a magnetic field in the direction of the propagation as well as a potential step.<sup>6</sup> In their setup, leads with negligible SOI and vanishing magnetic field as present in any experimental realization were not taken into account.

The goal of the present work is twofold. We *first* investigate, under which conditions spin-polarized currents through a *finite length* 1D wire with SOI and parallel magnetic field can be achieved, if the coupling to two semi-infinite *leads* is included. We study the influence of a potential step and a localized impurity. Such inhomogeneities play an important role for the spin polarization.

In the Datta-Das setup as well as in the system suggested by Strēda and Sēba the spin dependent transport properties heavily rely on the strictly 1D nature of the quantum wire with only one partially filled subband. Already in the presence of a few filled subbands the control over the spin ceases.<sup>7</sup> In a few hundred nanometers long strictly 1D wires the Coulomb repulsion of electrons is expected to have a dramatic effect on the physics.

Such systems cannot be described by Fermi liquid theory. Instead, the low-energy properties are captured by the *Luttinger liquid* phenomenology.<sup>8</sup> One can thus expect that electron correlations will also affect the performance of spintronic devices made of 1D wires.<sup>7,9,10,11</sup> In particular, local inhomogeneities, which are important to achieve controllable spin polarization in the Strēda and Sēba setup, strongly suppress the conductance in Luttinger liquids.<sup>12,13</sup> It is thus mandatory to investigate how the spin polarization is affected by Luttinger liquid physics. This is the *second* goal of our work. A first step in analyzing the performance of the Strēda and Sēba spin filter in the presence of the electron-electron interaction was taken in Ref. 14.

Standard methods such as the self-consistent Hartree-Fock approximation do not capture the Luttinger liquid physics of our setup and are known to lead to severe artifacts if being applied to low-dimensional electron systems with Coulomb interaction. We therefore use an approximation which is based on the functional renormalization group (fRG) approach to treat the two-particle interaction in a model Hamiltonian. In the absence of SOI, it was shown to be a reliable tool to calculate the linear conductance of inhomogeneous quantum wires for weak to intermediate interactions.<sup>15,16</sup>

We show that for vanishing two-particle interaction spin polarized currents can be obtained using a similar mechanism as in Ref. 6, even in the presence of nonmagnetic leads with vanishing SOI and zero magnetic field. We then include the Coulomb interaction in our analysis. We first consider short wires (several tens of nanometers) in which Luttinger liquid physics does not become apparent and investigate how the spin polarization is affected by the two-particle interaction. We find that it strongly modifies the energy regime (energy of the incoming particles) in which spin polarization can be achieved. Next, the focus is on system sizes for which Luttinger liquid behavior is apparent in the absence of SOI (wires of several hundreds of nanometers). In particular, we analyze if the

spin polarization of an inhomogeneous wire is suppressed as a function of an infrared energy scale. We find that although the total conductance shows a power-law suppression in the presence of SOI (similar to the situation with vanishing SOI) the polarization *does not* follow such a scaling law. We present indications that the degree of spin polarization in the presence of Coulomb interaction might even exceed the one obtained for vanishing two-particle interaction.

While in most studies on spintronic devices the correlations are neglected even if the suggested setups contain 1D quantum wires our results clearly reveal the importance of the two-particle Coulomb interaction in the spin filter suggested in Ref. 6. We here refrain from making direct contact to existing or future experiments as we are mainly interested in studying the basic physics within a simplified model. It must certainly be extended to be considered realistic. However, our parameters are taken from a physically sensible range (see below).

This paper is organized as follows. In the next section, we introduce our setup and lattice model. The techniques to obtain the linear conductance are described in Sect. III. In Sect. IV, we first present our results for spin-polarized transport at vanishing two-particle interaction in the presence of leads. We next include the Coulomb interaction and study its interplay with the SOI, the magnetic field, and external potentials. Our results are summed up in Sect. V.

## II. THE MODEL

### A. Spin-orbit interaction

The two prototypical experimental systems for strictly 1D quantum transport are carbon nanotubes and confined electron gases which form at the interface of properly designed semiconductor heterostructures. In the latter, the confining potential generically leads to a sizable SOI and these are the type of systems we have in mind in the following. But also in the former the SOI seems to be surprisingly large.<sup>17</sup> We choose our coordinate system such that the heterostructure confines the two-dimensional electron gas in  $z$ -direction and the external potential results in a confinement of the electrons in  $y$ -direction. Therefore, the electrons are able to move in  $x$ -direction only. Since we assume the confinement to be very sharp, the different electronic subbands will be well separated. For a sufficiently low electron density, we can thus focus on the lowest subband and neglect any subband mixing.

The sharp confinement leads to large electric fields, which induce a spin-orbit coupling<sup>18</sup>

$$H_{\text{SO}} = -\frac{e\hbar}{4m^2c^2}\boldsymbol{\sigma} \cdot \left[ \mathbf{E} \times \left( \mathbf{p} - \frac{e}{c}\mathbf{A} \right) \right] \quad (1)$$

with the electric field  $\mathbf{E} = -\nabla V/e$  ( $e < 0$  is the electron charge) being the gradient of the ambient poten-

tial. For the 1D infinite noninteracting continuum model (1D electron gas), SOI results in a horizontal splitting of the quadratic electron energy dispersion  $\epsilon(k, s)$  with wave number  $k$  and  $s = \pm$  being an additional quantum number. Within a certain parameter regime a magnetic field in  $x$ -direction, which couples to the electron spin, leads to a deformation of the lower parabolic branch resulting in a double well form (see the low-energy region of the two central dispersions of Fig. 1). Moreover, it was shown in Ref. 6 and extensively discussed in Ref. 19 that the spin expectation values become  $k$ -dependent and display a rich behavior in the presence of both SOI and magnetic field. Applying an additional step-like potential and considering electrons with energy in regions of only double degeneracy leads to the above mentioned spin-polarized transport.<sup>6,19</sup>

### B. Lattice system

The starting point of our investigation is a 1D noninteracting tight-binding lattice Hamiltonian. As our single-particle basis, we choose Wannier states  $|j, \sigma\rangle$  with  $j \in \{1, \dots, N\}$  labeling the lattice site and  $\sigma = \uparrow, \downarrow$  denoting the spin. The spin quantization is chosen along the  $z$ -direction. The Hamiltonian can be written as

$$H_0 = H_{\text{free}} + H_{\text{pot}} + H_R + H_Z, \quad (2)$$

with the free part

$$H_{\text{free}} = -t \sum_{j=1}^{N-1} \sum_{\sigma} \left( c_{j+1, \sigma}^\dagger c_{j, \sigma} + c_{j, \sigma}^\dagger c_{j+1, \sigma} \right), \quad (3)$$

describing the hopping of amplitude  $t > 0$  and the external potential (e.g. due to nano-device structuring)

$$H_{\text{pot}} = \sum_{j=1}^N \sum_{\sigma} V_{j, \sigma} c_{j, \sigma}^\dagger c_{j, \sigma}. \quad (4)$$

Here,  $c_{j, \sigma}^\dagger$  denotes the creation operator of an electron at site  $j$  with spin  $\sigma$ . In a lattice model the effect of SOI due to confinement in  $z$ -direction is accounted for by a spin-flip hopping,<sup>20</sup> and the effect of SOI due to confinement in  $y$ -direction by an imaginary spin-conserving hopping.<sup>19</sup> Thus the SOI (Rashba) term reads

$$H_R = - \sum_{j=1}^{N-1} \sum_{\sigma, \sigma'} \alpha_{z, j} \left( c_{j+1, \sigma}^\dagger (i\sigma_y)_{\sigma, \sigma'} c_{j, \sigma'} + \text{H.c.} \right) \\ + \sum_{j=1}^{N-1} \sum_{\sigma, \sigma'} \alpha_{y, j} \left( c_{j+1, \sigma}^\dagger (i\sigma_z)_{\sigma, \sigma'} c_{j, \sigma'} + \text{H.c.} \right). \quad (5)$$

The SOI coupling constants  $\alpha_{z, j} > 0$  and  $\alpha_{y, j} > 0$  are assumed to depend on the bond ( $j, j+1$ ) considered.<sup>21</sup> The effect of a magnetic field is captured by the Zeeman

term

$$H_Z = \gamma \sum_{j=1}^N \sum_{\sigma, \sigma'} B_j c_{j, \sigma}^\dagger \left[ (\sigma_x)_{\sigma, \sigma'} \sin \theta \cos \varphi \right. \\ \left. + (\sigma_y)_{\sigma, \sigma'} \sin \theta \sin \varphi + (\sigma_z)_{\sigma, \sigma'} \cos \theta \right] c_{j, \sigma'} , \quad (6)$$

with a site dependent magnetic field in (for now) arbitrary direction  $\mathbf{B}_j = B_j (\sin \theta \cos \varphi, \sin \theta \sin \varphi, \cos \theta)$ , and  $\gamma$  being the Zeeman coupling constant. For  $N \rightarrow \infty$  this lattice model was shown to give a similar low-energy dispersion as the continuum model as well as a similar energy dependence of the spin expectation values.<sup>19</sup>

We supplement our model by a local site-dependent Coulomb interaction  $U_{1,j}$

$$H_1 = \sum_{j=1}^N \sum_{\sigma, \sigma'} U_{1,j} c_{j, \sigma}^\dagger c_{j, \sigma} c_{j, \sigma'}^\dagger c_{j, \sigma'} (1 - \delta_{\sigma, \sigma'}) \quad (7)$$

and a bond-dependent nearest-neighbor Coulomb interaction  $U_{2,j}$

$$H_2 = \sum_{j=1}^{N-1} \sum_{\sigma, \sigma'} U_{2,j} c_{j+1, \sigma}^\dagger c_{j+1, \sigma} c_{j, \sigma'}^\dagger c_{j, \sigma'} \quad (8)$$

(extended Hubbard model). The total Hamiltonian of the quantum wire is given by

$$H = H_0 + H_1 + H_2. \quad (9)$$

At the sites 1 and  $N$  the 1D wire is (end-)coupled to two semi-infinite leads. Having in mind a possible experimental realization, we assume that the SOI in the leads is weak and can be neglected. Furthermore, the magnetic field is restricted to the wire region. We assume that after entering the leads the electrons are independent (Fermi liquid behavior in higher-dimensional systems). For a local lead-wire coupling and in the low-energy limit, only the leads' density of states at the end of the leads and at the chemical potential  $\mu$  (energy of incoming electrons) matters. For simplicity, we thus model the leads as semi-infinite 1D tight-binding chains ( $\chi = L, R$ )

$$H_\chi^{\text{lead}} = -\tilde{t}_\chi \sum_j \sum_\sigma \left[ d_{j+1, \sigma}^\dagger d_{j, \sigma} + \text{H.c.} \right], \quad (10)$$

with  $d_{j, \sigma}^\dagger$  being the creation operator of the leads,  $j = -\infty, \dots, 0$  for the left lead, and  $j = N+1, \dots, \infty$  for the right one. To prevent a proliferation of parameters we assume equal leads, set  $t_L = t_R = t$ , and measure all energies in units of the lead hopping  $t = 1$ . Our energy unit is therefore of the order of 1 eV. At the contacts, the electrons can tunnel in and out of the wire and the Hamiltonian of the wire-lead coupling is given by

$$H_{\text{coup}} = \sum_\sigma \left[ t_L c_{1, \sigma}^\dagger d_{0, \sigma} + t_R d_{N+1, \sigma}^\dagger c_{N, \sigma} + \text{H.c.} \right] \quad (11)$$

The site- and bond-dependence of  $\alpha_y, \alpha_z$ , the magnetic field, and the interaction matrix elements allows us to

adiabatically turn on and off these couplings over  $m_1$  lattice sites/bonds close to the wire-lead contacts. This will be done in order to prevent any unwanted electron backscattering from the contacts and is reminiscent of the gradual confinement to the 1D geometry in heterostructures. We emphasize that the precise shape of the weight function with which the couplings are turned on and off does not have any significant effect on the results as long as it is sufficiently smooth. In the bulk of the wire, these parameters reach constant values (for details, see below).

### III. METHODS

#### A. The linear conductance

Using the Landauer-Büttiker approach,<sup>22</sup> one can express the spin-dependent linear conductance  $G_{\sigma, \sigma'}$  for *vanishing two-particle interaction* in terms of the transmission  $\mathcal{T}_{\sigma\sigma'}(\varepsilon)$

$$G_{\sigma, \sigma'} = -\frac{e^2}{h} \int |\mathcal{T}_{\sigma, \sigma'}(\varepsilon)|^2 f'(\varepsilon) d\varepsilon \quad (12)$$

with  $f(\varepsilon)$  being the Fermi function. The indices  $\sigma, \sigma'$  denote the  $z$ -component of the electron spin before entering and after leaving the quantum wire, respectively. The spin is conserved outside the quantum wire, since we neglect any SOI in the leads as well as spin relaxation. Using the Feshbach projection,<sup>23</sup> it is easy to show that the transmission is connected to the  $(1, N)$  matrix element of the retarded single-particle Green's function  $\mathcal{G}^{\sigma, \sigma'}(\varepsilon + i0)$  of the entire system (including the leads)

$$\mathcal{T}_{\sigma, \sigma'}(\varepsilon) = 2t_L t_R \sin(k_\varepsilon) \mathcal{G}_{1, N}^{\sigma, \sigma'}(\varepsilon + i0) \quad (13)$$

with  $k_\varepsilon = \arccos(-\varepsilon/2)$ .

At  $T = 0$ , on which we focus from now on, the derivative of the Fermi function is a  $\delta$ -function and Eq. (12) simplifies to

$$G_{\sigma, \sigma'} = \frac{e^2}{h} |\mathcal{T}_{\sigma, \sigma'}(\mu)|^2, \quad (14)$$

with the chemical potential given by the Fermi momentum,  $\mu = -2 \cos k_F$ . For noninteracting leads, this relation holds even if the two-particle interaction in the wire is finite,<sup>24</sup> where  $\mathcal{G}$  in Eq. (13) is the *interacting* Green's function of the entire system. To compute the latter we first integrate out the leads by projection (see the next subsection) and treat the remaining interacting system of size  $N$  using the approximate fRG procedure.

Using standard Feshbach projection, the effect of the leads can be cast in energy dependent contributions to the  $(1, 1)$  and  $(N, N)$  matrix elements of the self-energy.<sup>23</sup> They read

$$\begin{aligned} (\Sigma_{\text{lead}})_{1,1}^{\sigma, \sigma'}(z) &= \delta_{\sigma, \sigma'} t_L^2 g(z), \\ (\Sigma_{\text{lead}})_{N,N}^{\sigma, \sigma'}(z) &= \delta_{\sigma, \sigma'} t_R^2 g(z) \end{aligned} \quad (15)$$

with the Green's function

$$g(z) = z + \mu \mp \sqrt{(z + \mu)^2 - 4} \quad (16)$$

of the semi-infinite leads taken at the first lattice site. The sign must be chosen such that  $\lim_{|z| \rightarrow \infty} g_{\sigma,\sigma}(z) = 0$ . In the following, we absorb the contribution of the leads to the self-energy into the noninteracting propagator  $\mathcal{G}_0$  of the wire. The full interacting Green's function is given by the Dyson equation

$$\mathcal{G} = (\mathcal{G}_0^{-1} - \Sigma)^{-1}. \quad (17)$$

## B. Functional renormalization group

We briefly describe the fRG method used here<sup>25</sup> to approximately compute  $\mathcal{G}$ .<sup>26,27</sup> Detailed accounts of the application of this method to inhomogeneous, interacting quantum wires have been given in the last few years.<sup>15,16</sup> Including the SOI and the magnetic field does only require minor extensions.

Starting point of the fRG scheme is the propagator  $\mathcal{G}_0$  which follows from the noninteracting Hamiltonian Eq. (2) and the self-energy contribution of the leads Eq. (15). It is supplemented with a cutoff  $\Lambda$  such that all modes with Matsubara frequencies  $|\omega| < \Lambda$  are suppressed, i.e.

$$\mathcal{G}_0^\Lambda(i\omega) = \Theta(|\omega| - \Lambda) \mathcal{G}_0(i\omega), \quad (18)$$

where  $\Lambda$  runs from  $\infty$  to 0. Inserting  $\mathcal{G}_0^\Lambda$  in the generating functional of the one-particle irreducible vertex functions, one obtains an infinite hierarchy of coupled differential equations for the vertex functions by differentiating the generating functional with respect to  $\Lambda$  and expanding it in powers of the external fields. To obtain a manageable set of flow equations, this hierarchy must be truncated. In a first step, we neglect the three-particle vertex  $\Gamma_3^\Lambda$ , since it is zero at  $\Lambda = \infty$  and is generated only from terms of third order in the two-particle vertex  $\Gamma^\Lambda$ , which are small as long as  $\Gamma^\Lambda$  does not become too large.

For arbitrary local  $U_1$ , nearest-neighbor interaction  $U_2$ , and filling  $n \in (0, 2)$  of the band, the flow of the two-particle vertex must be kept at least to lowest (that is second) order to correctly obtain the scaling behavior (for large  $N$ ) of correlation functions to leading order in the interaction. In the absence of SOI this is already known from the so-called ‘‘g-ology’’ model.<sup>28</sup> An RG analysis of this model shows that the two-particle scattering with momentum transfer  $2k_F$  of electrons with opposite spin, the so-called  $g_{1,\perp}$  term, flows to zero. If one is interested in correlation functions of large systems, this scaling must be captured by any sensible approximation. For the extended Hubbard model and vanishing SOI, this has been done in Ref. 16 using fRG. As the parameterization of the two-particle vertex used there relies on spin conservation, it cannot easily be extended to the present situation with SOI. Here, we are thus forced to proceed differently.

In the extended Hubbard model the coupling  $g_{1,\perp}$  is given by

$$g_{1,\perp} = U_1 + 2U_2 \cos(2k_F). \quad (19)$$

If it is zero initially, it will not get generated in a lowest-order RG analysis of the corresponding ‘‘g-ology’’ model (for vanishing SOI). If one is interested in the behavior of correlation functions to leading order in the interaction, the flow of the vertex can then be neglected altogether. A vanishing  $g_{1,\perp}$  is achieved, if we stick to parameters  $U_1$ ,  $U_2$ , and  $k_F$  such that the right hand side of Eq. (19) is zero. Neglecting terms of order  $U^2\alpha$ , where  $U$  stands for either  $U_1$  or  $U_2$  and  $\alpha$  for either  $\alpha_x$  or  $\alpha_y$  the same reasoning holds if the SOI is included. When studying the effect of the two-particle interaction for large systems (Luttinger liquid behavior in the scaling limit), we thus exclusively consider the case

$$U_2 = -U_1/[2 \cos(2k_F)] \quad (20)$$

and neglect the flow of the two-particle vertex. This assumption does not affect the asymptotic power-law scaling of the conductance for vanishing SOI.<sup>16</sup> We expect the same to hold for nonzero SOI and thus focussing on this situation does not present a severe constraint for our purposes. An fRG analysis of the flow of the two-particle vertex in the presence of SOI which would allow to investigate novel phases resulting from the interplay of the two-particle interaction and the SOI<sup>11</sup> is left for further studies.

For wires of the order of a hundred lattice sites, the flow of the components of the two-particle vertex is cut off on fairly large energy scales ( $\propto 1/N$ ), affects correlation functions (such as the single-particle Green's function we are aiming at) only weakly, and can thus be neglected even if one chooses parameters such that Eq. (20) does not hold. Our approximation contains at least all terms of first order perturbation theory in the two-particle interaction.<sup>15,16</sup>

Within these approximations the self-energy (negative of the one-particle vertex) becomes frequency independent<sup>15,16</sup>, and its flow equation reads

$$\frac{\partial}{\partial \Lambda} \Sigma_{1',1}^\Lambda = -\frac{1}{2\pi} \sum_{\omega=\pm\Lambda} \sum_{2,2'} e^{i\omega 0^+} \mathcal{G}_{2,2'}^\Lambda(i\omega) \Gamma_{1',2';1,2}, \quad (21)$$

where the indices  $1, 1', 2, 2'$  label the quantum numbers  $j, \sigma$  and

$$\mathcal{G}^\Lambda(i\omega) = [\mathcal{G}_0^{-1} - \Sigma^\Lambda]^{-1}. \quad (22)$$

One starts the numerical integration at a large initial value  $\Lambda_0 \sim 10^8$  and integrates down to  $\Lambda = 0$ . Following the description in Ref. 15, we add a one-particle potential  $\nu$  to the Hamiltonian  $H_1$  and  $H_2$ , such that the starting value of the self-energy, which accounts for the finite contribution resulting from the integration of Eq. (21) over

the interval  $(\infty, \Lambda_0]$ , vanish. The initial condition for  $\Lambda_0 \rightarrow \infty$  then reads

$$\Sigma_{1,1}^{\Lambda_0} = 0. \quad (23)$$

The self-energy  $\Sigma^{\Lambda=0}$  at the end of the flow can be considered as an approximation to the full self-energy. Using the Dyson equation (17), the Green's function entering the expression for the  $T = 0$  linear conductance can be computed.

For our model with only local and nearest neighbor interactions the self-energy is a tridiagonal matrix in the Wannier basis states, with each entry being a  $2 \times 2$  matrix in spin space. As  $\Sigma$  is frequency independent within our approximation, its matrix elements can be interpreted as the interaction induced renormalizations of the parameters of the noninteracting model. Depending on the matrix element considered these are the SOI and spin conserving hoppings, magnetic fields as well as on-site potentials all being position dependent.<sup>15,16</sup> This implies that to approximately obtain the  $T = 0$  conductance of an interacting system the Green's function of an effective noninteracting problem with renormalized parameters must be computed. This is similar to the Hartree-Fock approximation. However, we emphasize that in our approximate fRG a different class of diagrams is resummed, this way avoiding the artifacts known to emerge if the Hartree-Fock approximation is used for problems of interacting electrons in low dimensions.

For half filling ( $n = 1$ ), the electron correlations drive our system towards a Mott insulator state (details depend on the parameters  $U_1$  and  $U_2$ ), which becomes of relevance for sufficiently large  $N$ .<sup>8</sup> As we are here interested in spin dependent transport through *metallic* wires we only consider fillings away from  $n = 1$  when studying large  $N$ .<sup>29</sup>

#### IV. RESULTS

Following the steps described in the last section, we calculate the spin resolved linear conductance  $G_{\sigma,\sigma'}$  with  $\sigma, \sigma = \uparrow, \downarrow$  (with respect to the  $z$ -direction), as a function of the system's chemical potential  $\mu$  (energy of incoming electrons) and the system size  $N$ . The total conductance is given by the sum of the four components

$$G_{\text{total}} = G_{\uparrow\uparrow} + G_{\uparrow\downarrow} + G_{\downarrow\uparrow} + G_{\downarrow\downarrow}. \quad (24)$$

As our leads are free of SOI, the definition of the spin polarization does not involve the spin expectation value. This has to be contrasted to the definition of Ref. 6 for a system without leads. Due to the choice of the  $z$ -axis as the spin quantization axis, the spin polarization in  $z$ -direction can be defined as the “normalized” difference between the probability that an electron enters the right lead with spin up and the probability that it enters with spin down

$$P_z = \frac{G_{\uparrow\uparrow} + G_{\downarrow\uparrow} - G_{\uparrow\downarrow} - G_{\downarrow\downarrow}}{G_{\text{total}}}. \quad (25)$$

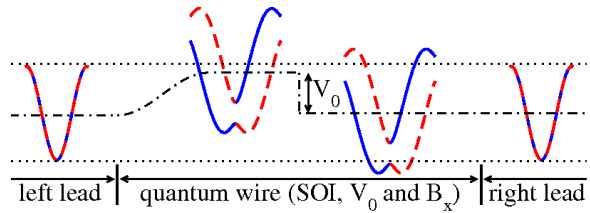


FIG. 1: (Color online) Sketch of the system with SOI and parallel magnetic field in the wire. The leads have a cosine-like dispersion, whereas the “local” dispersion in the quantum wire has two nondegenerate branches [ $s = +$  (solid line),  $s = -$  (dashed line)]. A potential step which is turned on smoothly at the left contact and turned off sharply in the middle of the wire is indicated by the dashed-dotted line. The energies of the incoming and outgoing electrons are confined within the dotted lines.

The conductance components and spin polarization in the  $x$ - and  $y$ -direction can be obtained by a simple base transformation. The transmissions which need to be inserted into Eq. (14) are

$$\begin{aligned} \mathcal{T}_{\uparrow\uparrow}^{(x)} &= (\mathcal{T}_{\uparrow\uparrow} + \mathcal{T}_{\uparrow\downarrow} + \mathcal{T}_{\downarrow\uparrow} + \mathcal{T}_{\downarrow\downarrow}) / 2, \\ \mathcal{T}_{\uparrow\downarrow}^{(x)} &= (\mathcal{T}_{\uparrow\uparrow} - \mathcal{T}_{\uparrow\downarrow} + \mathcal{T}_{\downarrow\uparrow} - \mathcal{T}_{\downarrow\downarrow}) / 2, \\ \mathcal{T}_{\downarrow\uparrow}^{(x)} &= (\mathcal{T}_{\uparrow\uparrow} + \mathcal{T}_{\uparrow\downarrow} - \mathcal{T}_{\downarrow\uparrow} - \mathcal{T}_{\downarrow\downarrow}) / 2, \\ \mathcal{T}_{\downarrow\downarrow}^{(x)} &= (\mathcal{T}_{\uparrow\uparrow} - \mathcal{T}_{\uparrow\downarrow} - \mathcal{T}_{\downarrow\uparrow} + \mathcal{T}_{\downarrow\downarrow}) / 2 \end{aligned} \quad (26)$$

and

$$\begin{aligned} \mathcal{T}_{\uparrow\uparrow}^{(y)} &= (\mathcal{T}_{\uparrow\uparrow} - i\mathcal{T}_{\uparrow\downarrow} + i\mathcal{T}_{\downarrow\uparrow} + \mathcal{T}_{\downarrow\downarrow}) / 2, \\ \mathcal{T}_{\uparrow\downarrow}^{(y)} &= (-i\mathcal{T}_{\uparrow\uparrow} + \mathcal{T}_{\uparrow\downarrow} + \mathcal{T}_{\downarrow\uparrow} + i\mathcal{T}_{\downarrow\downarrow}) / 2, \\ \mathcal{T}_{\downarrow\uparrow}^{(y)} &= (i\mathcal{T}_{\uparrow\uparrow} + \mathcal{T}_{\uparrow\downarrow} + \mathcal{T}_{\downarrow\uparrow} - i\mathcal{T}_{\downarrow\downarrow}) / 2, \\ \mathcal{T}_{\downarrow\downarrow}^{(y)} &= (\mathcal{T}_{\uparrow\uparrow} + i\mathcal{T}_{\uparrow\downarrow} - i\mathcal{T}_{\downarrow\uparrow} + \mathcal{T}_{\downarrow\downarrow}) / 2, \end{aligned} \quad (27)$$

where  $\mathcal{T}_{\sigma,\sigma'}$  denotes the transmission with respect to the  $z$ -direction. The corresponding polarizations follow as in Eq. (25) with  $G$  replaced by  $G^{(x)}$  and  $G^{(y)}$ , respectively.

#### A. Vanishing Coulomb interaction

##### 1. A potential step

To investigate whether spin polarized currents can be achieved using a mechanism similar to that of Ref. 6 in the presence of nonmagnetic leads, we consider a setup that is close in spirit to the one studied there. We therefore add a potential step to the wire which can be used to shift the energy into the region of only doubly-degenerate states as sketched in Fig. 1. To prevent any backscattering at the left contact it is turned on smoothly there

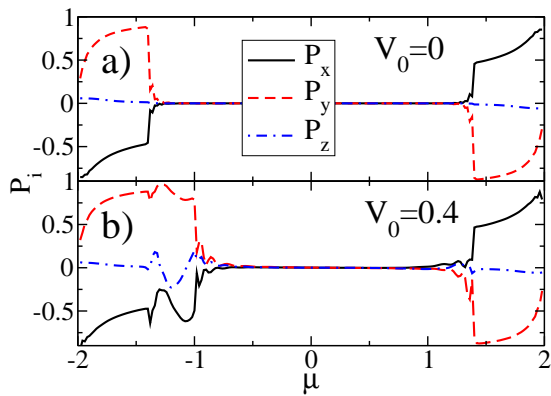


FIG. 2: (Color online) Spin polarization in  $x$ -,  $y$ - and  $z$ -direction as a function of  $\mu$  for a homogeneous system [ $V_0 = 0$ , a)] and a system with potential step [ $V_0 = 0.4$ , b)] for system parameters  $N = 100, m_1 = 20, t_L = t_R = 1, \alpha_y = 0, \alpha_z = 0.8$ , and  $\gamma B_x = 0.6$ . Inside the region with two conducting channels, there is no significant spin polarization. The high and low energy polarization is independent from  $V_0$  in good approximation. The potential leads to effects for  $\mu \in [-2 + \gamma B_x, -2 + \gamma B_x + V_0]$ .

and turned off sharply in the middle of the wire (dashed-dotted line in Fig. 1). Due to the smooth variation of the system parameters at the left contact, the cosine-like dispersion of the leads is “adiabatically” transformed into the “local” dispersion in the wire. A similar “adiabatic” transition occurs at the right contact. As the achieved wire dispersion is an essential ingredient of the spin filter to perform properly,<sup>6,19</sup> modelling a smooth variation at the contacts is mandatory. However, assuming a gradual crossover from higher-dimensional leads to the 1D wire appears to be quite natural in heterostructures.

Fig. 2 shows the spin polarization  $P_i$ ,  $i = x, y, z$ , for a homogeneous system [ $V_0 = 0$ , Fig. 2a)] and a system with potential step [ $V_0 = 0.4$ , Fig. 2b)] for system parameters  $N = 100, m_1 = 20, \alpha_y = 0, \alpha_z = 0.8$ , and  $\gamma B_x = 0.6$ . We chose the value for  $\alpha_z$  to be larger than the spin-orbit parameter  $\alpha \sim 0.1$  eV extracted from Ref. 30 for bulk InAs, since the SOI is significantly increased in semiconductor heterostructures. The lead-wire tunnel contacts modelled by  $t_{L/R}$  are assumed to be “perfect”  $t_L = t_R = 1$ , a situation on which we focus from now on. The curves show a large spin polarization in  $x$ - and  $y$ -direction for  $\mu \notin [-2 + \gamma B_x + V_0, 2 - \gamma B_x]$ , i.e. as long as there is only one conducting channel. This polarization is a “trivial” band effect due to the Zeeman splitting. Without SOI, one obtains a perfect spin-polarization in  $x$ -direction,  $P_x = \pm 1$ , in this interval [see Fig. 3a)]. For finite SOI, the spin is rotated out of the  $x$ -direction leading to non-vanishing components  $P_y$  and  $P_z$ . Similarly to the continuum situation,<sup>19</sup>  $\alpha_z$  ( $\alpha_y$ ) mainly leads to a spin rotation into the  $y$ - ( $z$ -) direction.

The most interesting energy regime in connection with Ref. 6 is  $\mu \in [-2 + \gamma B_x, -2 + \gamma B_x + V_0]$  in Fig. 2b). In this interval of width  $V_0$ , we observe nonvanishing, but

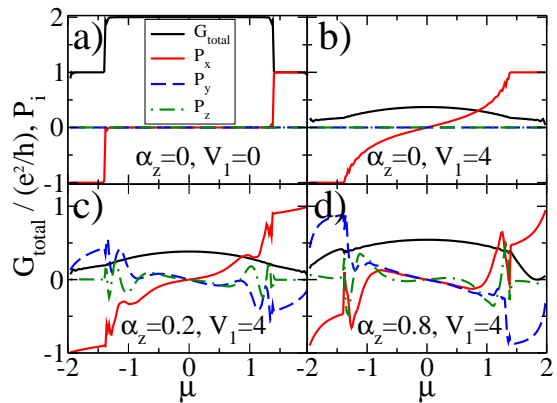


FIG. 3: (Color online) Conductance and spin polarization for a system of  $N = 101$  lattice sites ( $m_1 = 20$ ) with a single impurity  $V_1$  in the middle of the system in presence of a magnetic field  $\gamma B_x = 0.6$  and different SOI couplings  $\alpha_z$  ( $\alpha_y = 0$ ). a) The homogeneous system shows a perfect step-like polarization in  $x$ -direction. b) The shape of  $P_x$  is washed out in presence of a strong single impurity  $V_1 = 4$  and the conductance is severely decreased. c) Small SOI coupling  $\alpha_z = 0.2$  leads to finite  $P_y, P_z$  and polarization oscillations. d) The oscillations are enhanced by increasing  $\alpha_z$ .

strongly oscillating components of the polarization. The oscillations can be traced back to those of the conductance components and are absent in the continuum model of Ref. 6. By a mechanism similar to the one discussed in Ref. 6, we obtain a nonvanishing polarization. As was pointed out in Ref. 19 for the lead-less continuum model, the polarization  $P_x$  (in  $x$ -direction) only depends on the absolute value  $\alpha$  and not on the direction of the effective SOI field and  $|P_y/P_z| = |\alpha_z/\alpha_y|$ . Averaging over the polarization oscillations, this holds in very good approximation also for the lattice model with leads, although the polarization here is defined by Eq. (25) and not in terms of spin expectation values.<sup>6</sup> Because of the large oscillations (absent in the lead-less continuum model) the spin polarization reacts very sensitive to changes in the chemical potential  $\mu$ . This could be of interest to control the spin polarization in future spintronic devices.

## 2. A single impurity

Another interesting polarization effect occurs, if we insert a localized impurity of strength  $V_1$  in our system with SOI and parallel magnetic field. The exact position of the impurity within the bulk part of the wire does not matter and we here locate it in the middle of the wire.

Fig. 3 shows the conductance and spin polarization of a system with  $N = 101$  lattice sites ( $m_1 = 20$ ) with a single impurity  $V_1$  for a magnetic field  $\gamma B_x = 0.6$  and different SOI couplings  $\alpha_z$  ( $\alpha_y = 0$ ). The system without SOI and without any impurity ( $V_1 = 0$ ) shows a perfect step-like polarization in  $x$ -direction (“trivial” band effect), whereas  $P_y = P_z = 0$  [see Fig. 3a)]. The step

is smeared out and  $P_x$  can be tuned smoothly in presence of an intermediate to strong single impurity  $V_1 = 4$  while the total conductance is severely decreased in this case [see Fig. 3b)]. For small SOI,  $\alpha_z = 0.2$ ,  $P_x$  is still the dominant polarization component, but  $P_y$  and  $P_z$  become finite. All polarization components show oscillations for  $\mu \in [-2 + \gamma B_x, 2 - \gamma B_x]$ , which become heavily pronounced at the edges of this interval [see Fig. 3c)]. For large SOI [see Fig. 3d)],  $\alpha_z = 0.8$ , we observe the same behavior for  $\mu \notin [-2 + \gamma B_x, 2 - \gamma B_x]$  as in the impurity-free case [see Fig. 2a)] with  $P_z$  playing only a minor role. The oscillations of the polarization components are more pronounced compared to the case with small  $\alpha_z$ , especially for  $P_x$ . Moreover, the total conductance is enlarged due to the smaller ratio of  $V_1$  and the effective hopping  $\sqrt{t^2 + \alpha_z^2}$ . Due to the large oscillations, each spin polarization component reacts very sensitive to changes in  $\mu$  and can therefore be tuned by adjusting  $\mu$ .

In this section we studied systems with  $N \sim \mathcal{O}(10^2)$  lattice sites, corresponding to wires of the order of tens of nanometers. For vanishing two-particle interaction increasing the number of lattice sites does not affect the results obtained here.

### B. The effect of the Coulomb interaction

We now add the terms  $H_1$  and  $H_2$  given in Eqs. (7) and (8) to our Hamiltonian and use the fRG to approximately compute the conductance. We first study short quantum wires with  $N \sim \mathcal{O}(10^2)$  lattice sites and investigate how the energy regime (of the incoming electrons) in which spin polarized currents can be obtained is modified by the Coulomb interaction. Changes can be traced back to the interaction induced renormalization of the parameters of the noninteracting model.<sup>31</sup>

In a second step we focus on a fixed chemical potential, at which spin polarization is observed and study how this is modified if the system size  $N$  is increased. The inverse of  $N$ , more precisely  $\delta \propto v_F/N$  (with the Fermi velocity  $v_F$ ), presents an infrared energy scale in our setup. In the absence of SOI and a magnetic field, inhomogeneities, such as single impurities and potential steps, are known to lead to a power-law suppression of the conductance as a function of infrared energy scales.<sup>12,13,15,16</sup> We demonstrate that while the total conductance shows a similar behavior for finite SOI, the polarization does not display scaling behavior.

To model a gradual transition from a higher-dimensional to a 1D system at the lead-wire contacts, we gradually increase  $U_1$  and  $U_2$  over  $m_1$  lattice sites starting at the contacts. This prevents electron backscattering at the contacts due to the inhomogeneous two-particle interaction and one achieves unitary total conductance in the absence of an external single-particle potential. As the details of the variation of the interaction do not matter as long as it is sufficiently smooth,<sup>32</sup> we chose the same weight function as for the single-particle param-

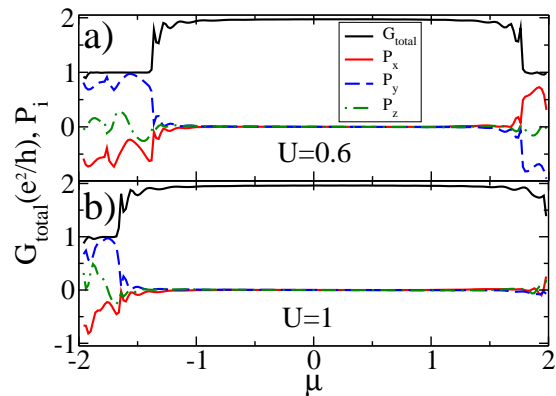


FIG. 4: (Color online) Total conductance and spin polarization as a function of the chemical potential  $\mu$  for a system with  $N = 100$  lattice sites ( $m_1 = 20$ ), potential step  $V_0 = 0.4$ , magnetic field  $\gamma B_x = 0.6$  and different Coulomb interaction  $U = U_1 = 2U_2$ . Increasing the Coulomb interaction [from a) to b)] for constant SOI  $\alpha_z = 0.8$  ( $\alpha_y = 0$ ) leads to a broadening of the energy regime with two open conducting channels. The spin polarization vanishes in this regime, but reveals a strong dependence on  $\mu$  in the regime with only one conducting channel.

eters. For an increasing chain length, the number of lattice sites over which the two-particle interaction and the single-particle parameters are turned on and off close to the contacts must be increased.<sup>32</sup>

#### 1. Short wires

Fig. 4 shows the total conductance and spin polarization as a function of the chemical potential  $\mu$  for a system with the same parameters as in Fig. 2b) but for nonvanishing Coulomb interaction. We consider a constant ratio of local and nearest-neighbor interaction,  $U_1/U_2 = 2$  (which appears to be a rather physical value), denote the local interaction  $U_1$  by  $U$  and study its affect on  $G_{\text{total}}$  and  $P_i$ ,  $i = x, y, z$ . Comparing Figs. 2b), 4a) and 4b), one notes that an increase of  $U$  leads to a broadening of the energy regime with two open conducting channels, that is “perfect” conductance  $G_{\text{total}} \approx 2e^2/h$ , and vanishing spin polarization. The Coulomb interaction thus leads to a decrease of the energy range in which spin polarization can be achieved. We emphasize, that within our approximation the above behavior can be understood in terms of transport through a quantum wire with *vanishing* two-particle interaction, but renormalized single-particle parameters (regular and spin-flip hoppings, magnetic field, and on-site potentials all of them depending on the lattice site index  $j$ ) given by the self-energy at the end of the fRG flow.<sup>31</sup>

We now investigate the influence of the Coulomb interaction on the transport properties of a short wire with a single impurity  $V_1$  in the middle of the quan-



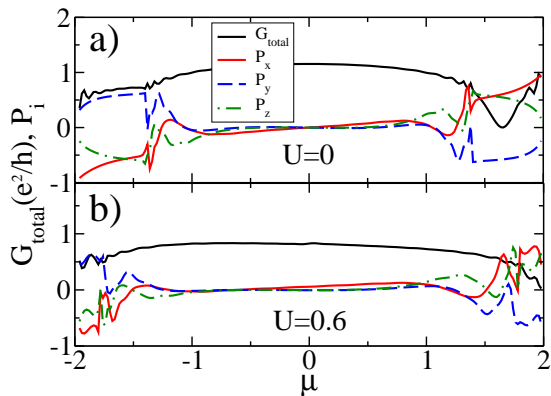


FIG. 5: (Color online) Total conductance and spin polarization components for a system with  $N = 101$  lattice sites ( $m_1 = 20$ ), SOI coupling parameters  $\alpha_y = \alpha_z = 0.5$ , magnetic field in  $x$ -direction,  $\gamma B_x = 0.6$ , and a single impurity  $V_1 = 2$  in the middle of the system. Increasing [from a) to b)] the two-particle interaction  $U$  leads to an increase of the energy regime with two conduction channels, but an overall decrease of the total conductance.

tum wire. Fig. 5 shows the total conductance  $G_{\text{total}}$  and polarization components  $P_i$ ,  $i = x, y, z$ , for a system with  $N = 101$  lattice sites ( $m_1 = 20$ ), SOI parameters  $\alpha_y = \alpha_z = 0.5$  and magnetic field  $\gamma B_x = 0.6$  in  $x$ -direction for  $V_1 = 2$ . Increasing the Coulomb interaction, we observe two tendencies. The first one is the increase of the energy regime with two conduction channels already found in the presence of the potential step. As the electrons scatter off the single impurity this does not lead to unitary conductance in the present case (in contrast to the case of a potential step). The second effect is an overall decrease of the total conductance with increasing  $U$ . This was to be expected as it is known that the effective strength of inhomogeneities increases in the presence of Coulomb correlations, eventually leading to power-law suppression for sufficiently large  $N$  (that is sufficiently small energies  $\delta$ ).<sup>12,13,15,16</sup>

For the fairly short wires studied in this subsection, results from first order perturbation theory in the two-particle interaction (for the self-energy) lead to qualitatively similar results as those obtained by our approximate fRG scheme. This does no longer hold for the longer wires studied next (Luttinger liquid behavior).

## 2. Luttinger liquid behavior in long wires

In the absence of SOI and a magnetic field, the linear conductance of a Luttinger liquid wire with a single impurity  $V_1$  is known to show power-law suppression as a function of an infrared energy scale (e.g. the temperature or  $\delta \propto v_F/N$ ), provided the latter is sufficiently small (scaling regime).<sup>12,13,15,16</sup> Surprisingly  $G_{\text{total}}$  vanishes in the asymptotic low-energy limit even for small  $V_1$ . However, the energy scale beyond which scaling holds de-

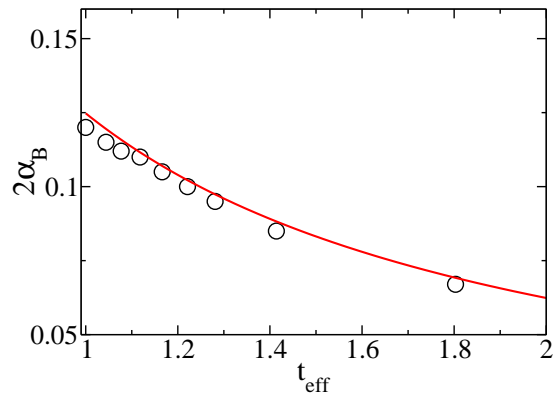


FIG. 6: (Color online) Dependence of the scaling exponent on the strength of the SOI (varying  $\alpha_y$  as well as  $\alpha_z$ ) for  $U = 0.3$  and filling  $n = 0.75$ . The circles are the data extracted from fitting  $G_{\text{total}}(\delta)$  by a power law for systems of a few thousand lattice sites. The error is of the order of the symbol size. The effective hopping  $t_{\text{eff}}$  depends on  $\alpha_y$  as well as  $\alpha_z$  and is defined in Eq. (30). The line shows the analytic expression Eq. (28) with  $t \rightarrow t_{\text{eff}}$ . The systematic deviation of the fRG data from the analytic expression can be explained by higher order corrections in  $U$  included in the numerical data, but not in Eq. (28)

pends on  $V_1$  and becomes exponentially small for small  $V_1$ , implying that exponentially long chains must be studied to observe power-law behavior. The scaling exponent is a function of the interaction and the filling, but is independent of the strength of the bare impurity.<sup>12,13,15,16</sup> For the extended Hubbard model and our choice of the ratio  $U_1/U_2 = U/U_2 = -2 \cos(2k_F)$  (vanishing two-particle backscattering  $g_{1\perp}$ ; see Sect. III B) it is given by

$$2\alpha_B = -\frac{\mu^2 - 4 \cos(\pi n)}{(2 - \mu^2)(2\pi t \sin(\pi n/2))} U \quad (28)$$

to leading order in  $U$ .<sup>16</sup> It was shown earlier that the approximate fRG procedure captures this power-law behavior and correctly reproduces the scaling exponent to order  $U$ .<sup>15,16</sup> In order to be able to compare our results to Eq. (28) we need to know  $n$  and therefore tune the additional one-particle potential  $\nu(U, \mu)$ , introduced in Sect. III B, such that the filling of the 1D quantum wire with electrons in presence of  $U_1$  and  $U_2$  corresponds to the filling  $n = 2 \arccos(-\mu/2)/\pi$  of the noninteracting leads at given  $\mu$ . Following Ref. 16, the starting values of the self-energy at lattice site  $j$  due to integration of the flow equations from  $\infty$  down to  $\Lambda_0$  are given by

$$\begin{aligned} \Sigma_{j,j'}^{\sigma\sigma';\Lambda_0} &= \left( \frac{1}{2}U_{1,j} + 2U_{2,j} \right) \delta_{j,j'} \delta_{\sigma,\sigma'}, \quad j \in \{2, \dots, N-1\}, \\ \Sigma_{j,j'}^{\sigma\sigma';\Lambda_0} &= \left( \frac{1}{2}U_{1,j} + U_{2,j} \right) \delta_{j,j'} \delta_{\sigma,\sigma'}, \quad j = 1, N, \end{aligned} \quad (29)$$

up to corrections of order  $1/\Lambda_0$ .

We first investigate if power-law scaling in the presence of a single impurity is also found for nonvanishing



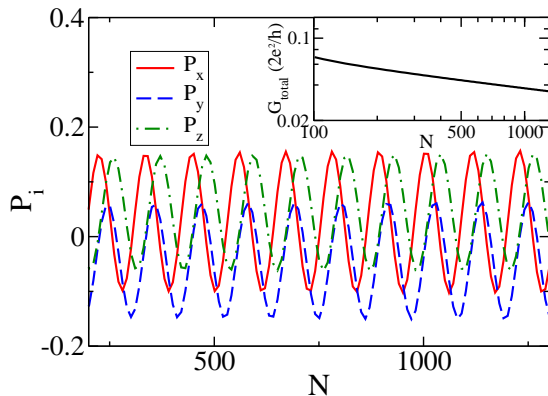


FIG. 7: (Color online) Main plot: Dependence of the polarization on the system size  $N$  for  $V_1 = 8$ ,  $\alpha_y = \alpha_z = 0.5$ ,  $\gamma B_x = 0.6$ ,  $n = 0.9$ , and  $U = 0.8$ . Inset: The total conductance as a function of  $N$  on a log-log scale. The parameters are as in the main plot.

SOI, but zero magnetic field, a situation in which no spin polarization is found. To this end we compute the total conductance as a function of  $\delta \propto v_F/N$  for fixed (small)  $U \lesssim 1$  (range of applicability of our approximate fRG procedure), fixed filling  $n \neq 1$  (see the discussion in Sect. III B), fixed SOI, and fixed intermediate to large  $V_1$  [such that the scaling regime is reached for  $N \sim \mathcal{O}(10^3)$ ]. The data for  $G_{\text{total}}(\delta)$  can be fitted by a power-law and we extract the asymptotic exponent. An example of the power-law behavior (as a function of  $N \sim \delta^{-1}$ ) in the case of an additional magnetic field is shown in the inset of Fig. 7. The scaling exponent depends on the SOI via an effective renormalized spin conserving hopping

$$t_{\text{eff}} = \sqrt{\alpha_y^2 + \alpha_z^2 + t^2}, \quad (30)$$

that is, the dependence of  $2\alpha_B$  is given by Eq. (28) with  $t$  replaced by  $t_{\text{eff}}$ . This is shown in Fig. 6 for  $U = 0.3$ ,  $n = 0.75$ , and different  $\alpha_y$  as well as  $\alpha_z$ . The systematic deviation of the data from the analytic expression (28) with  $t \rightarrow t_{\text{eff}}$  can be explained by higher order corrections in  $U$  included in the numerical data, but not in Eq. (28). The error of the fRG exponents extracted from fitting  $G_{\text{total}}(\delta)$  for systems of a few thousand lattice sites is of the order of the symbol size.

Next we consider the case of a single impurity in the presence of SOI and a magnetic field in  $x$ -direction, a situation with nonvanishing polarization (see the discussion in Sec. IV A 2). The main part of Fig. 7 shows the  $N \sim \delta^{-1}$  dependence of the three components of the polarization for  $V_1 = 8$ ,  $\alpha_y = \alpha_z = 0.5$ ,  $\gamma B_x = 0.6$ ,  $n = 0.9$ , and  $U = 0.8$ . In the inset we present the corresponding total conductance on a log-log-scale. While the latter shows a clear indication of power-law suppression, the polarization oscillates with a constant amplitude  $A_{\text{osc}}$ . A similar oscillation is found for  $U = 0$ . In fact, the amplitude of the oscillation shows a nonmonotonic dependence on  $U$ . Starting from  $U = 0$ , it first decreases

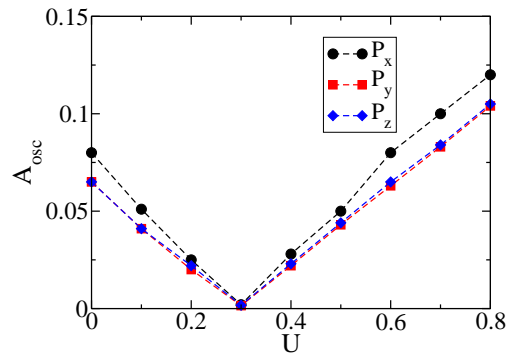


FIG. 8: (Color online) Amplitudes  $A_{\text{osc}}$  of the oscillations of the three components of the polarization (see main part of Fig. 7) as a function of the two-particle interaction  $U$  for the same parameters as in Fig. 7. Because of  $\alpha_y = \alpha_z$ , the amplitudes of the polarization in  $y$ - and  $z$ -direction are supposed to be the same. The discrepancy of these two data sets thus gives an estimate how accurately the amplitude can be read off from the numerical data.

linearly with increasing  $U$  up to  $U = 0.3$ , but increases for  $U > 0.3$  (see Fig. 8). For  $U = 0.8$  as shown in Fig. 7 the amplitude is roughly a factor of 1.5 larger than in the noninteracting case. Fig. 5 indicates that the details of this behavior depend on the filling (chemical potential of the incoming electrons). The above result implies that although the total current through (total linear conductance of) a quantum wire with a single impurity, SOI, and a magnetic field in the direction of the wire is generically strongly reduced as a function of  $N$  in the presence of the Coulomb interaction, the degree of spin polarization of the current stays constant. We note that the increase of  $A_{\text{osc}}$  as a function of  $U$  (see Fig. 8) has to be considered with caution as our approximation is only valid for sufficiently small  $U$ , while the increased polarization (compared to the noninteracting one) requires a small to intermediate  $U$ . It would thus be important to investigate the polarization using alternative methods. We verified that the exponent of the power-law suppression of  $G_{\text{total}}(\delta)$  is independent of  $\gamma B_x$  and thus to leading order in  $U$  given by Eq. (28) with  $t$  replaced by  $t_{\text{eff}}$ .

It would now be very interesting to investigate the scaling of the conductance and the dependence of the polarization on the length of the quantum wire for the setup with a potential step.<sup>6</sup> Unfortunately, it turns out that the relevant  $2k_F$ -scattering component of the potential step which is turned on adiabatically at the left contact but is turned off abruptly in the middle of the wire with a step height of a few ten percent of the band width is fairly small. We thus cannot reach the scaling regime for the accessible system sizes of order  $10^3$  to  $10^4$ . For larger step height the physics is dominated by “trivial” band effects we are not interested in. As for weak (local) single impurities the total conductance in the presence of the potential step decreases weakly with increasing  $N$  (no power-law scaling at the corresponding  $\delta$ ) while the components of the polarization oscillate with  $N$  with an

amplitude which is constant. One can enhance the effect of the potential step (the size of the  $2k_F$ -scattering component) by adding a (sufficiently strong) single impurity located in the middle of the system. For this combined inhomogeneity we observe exactly the same behavior as shown in Fig. 7 for a pure (strong) single impurity. Having this in mind we conjecture that a potential step with a sufficient large step size not limited by the finite band width will have the same effect on the total conductance (power-law suppression with length of wire) and the spin polarization (oscillation with an amplitude independent of the wire length) as a single localized impurity.

## V. SUMMARY

We have investigated the effect of SOI, a magnetic field and the Coulomb interaction on the transport properties of a 1D quantum wire attached to two semi-infinite non-interacting and nonmagnetic leads. Motivated by analytical calculations for a lead-less, noninteracting system described by a continuum model,<sup>6,19</sup> we have constructed a corresponding lattice model. The combined effect of SOI and a magnetic field led to a spin polarization which could be varied over a wide range in the presence of inhomogeneities (single impurity, potential step) by adjusting the energy of the incoming electrons (chemical potential).

Using the fRG, we were able to include the Coulomb

interaction in our system. We distinguished the cases of short quantum wires (of the order of a few tens of nanometers) and long ones (scaling regime; a few hundred nanometers). For short wires, we showed that the energy regime for which spin polarization can be found strongly depends on the Coulomb interaction and might even become very small depending on the other system parameters. For long wires the well-known power-law suppression of the total conductance of an inhomogeneous Luttinger liquid as a function of the system size was obtained with a scaling exponent which depends on the two-particle interaction, the filling (both as for vanishing SOI), but also on the strength of the SOI via an effective nearest-neighbor hopping. However, the spin polarization as a function of system size exhibited oscillations with constant amplitude, not signaling any suppression on low energy-scales (that is for large system sizes). We found indications that the amplitude of the oscillations and thus the degree of spin-polarization, might even become larger than for vanishing Coulomb interaction.

Our results indicate the importance of the two-particle Coulomb interaction in the spin filter suggested in Ref. 6. In most studies on spintronic devices these correlations are neglected even if the suggested setups contain 1D quantum wires. Obtaining a deeper understanding of the performance of 1D spin filters within more realistic models of interacting electrons presents a challenge for future theoretical studies.

- 
- <sup>1</sup> M.N. Baibich, J.M. Broto, A. Fert, F. Nguyen Van Dau, F. Petroff, P. Etienne, G. Creuzet, A. Friederich, and J. Chazelas, *Phys. Rev. Lett.* **61**, 2472 (1988).
- <sup>2</sup> G. Binasch, P. Grünberg, F. Saurenbach, and W. Zinn, *Phys. Rev. B* **39**, 4828(R) (1989).
- <sup>3</sup> S. Datta and B. Das, *Appl. Phys. Lett.* **56**, 7 (1990).
- <sup>4</sup> J.C. Egues, C. Gould, G. Richter, and L.W. Molenkamp, *Phys. Rev. B* **64**, 195319 (2001).
- <sup>5</sup> C.W.J. Beenakker, *Phys. Rev. B* **73**, 201304(R) (2006).
- <sup>6</sup> P. Strěda and P. Šěba, *Phys. Rev. Lett.* **90**, 256601 (2003).
- <sup>7</sup> M. Governale and U. Zülicke, *Phys. Rev. B* **66**, 073311 (2002); *Solid State Com.* **131**, 581, (2004).
- <sup>8</sup> For a recent review on LL physics see K. Schönhammer in *Strong Interactions in Low Dimensions*, Eds.: D. Baeriswyl and L. Degiorgi, Kluwer Academic Publishers, Dordrecht (2005).
- <sup>9</sup> W. Häusler, *Phys. Rev. B* **63**, 121310(R) (2001).
- <sup>10</sup> A. Iucci, *Phys. Rev. B* **68**, 075107 (2003).
- <sup>11</sup> V. Gritsev, G.I. Japaridze, M. Pletyukhov, and D. Baeriswyl, *Phys. Rev. Lett.* **94**, 137207 (2005).
- <sup>12</sup> C.L. Kane and M.P.A. Fisher, *Phys. Rev. Lett.* **68**, 1220 (1992); *Phys. Rev. B* **46**, 7268 (1992); *Phys. Rev. B* **46**, 15233 (1992).
- <sup>13</sup> A. Furusaki and N. Nagaosa, *Phys. Rev. B* **47**, 4631 (1993).
- <sup>14</sup> P. Devillard, A. Crépieux, K.I. Imura, and T. Martin, *Phys. Rev. B* **72**, 041309(R) (2005).
- <sup>15</sup> T. Enss, V. Meden, S. Andergassen, X. Barnabé-Thériault, W. Metzner, and K. Schönhammer, *Phys. Rev. B* **71**, 155401 (2005).
- <sup>16</sup> S. Andergassen, T. Enss, V. Meden, W. Metzner, U. Schollwöck, and K. Schönhammer, *Phys. Rev. B* **73**, 045125 (2006).
- <sup>17</sup> F. Kuemmeth, S. Ilani, D.C. Ralph, and P.L. McEuen, *Nature* **452**, 448 (2008).
- <sup>18</sup> R. Winkler, *Spin-Orbit Coupling Effects in Two-Dimensional Electron and Hole Systems*, Springer-Verlag, Berlin (2003).
- <sup>19</sup> J.E. Birkholz and V. Meden, *J. Phys.: Condens. Matter* **20**, 085226 (2008).
- <sup>20</sup> F. Mireles and G. Kirczenow, *Phys. Rev. B* **64**, 024426 (2001).
- <sup>21</sup> The SOI parameters are given by  $\alpha_i = eE_i/(4mc^2)$ ,  $i = y, z$ , with  $e$  being the (negative) electron charge and  $m$  the effective mass.<sup>19</sup> The electric field  $E_i$  as the gradient of the confining scalar potential is chosen to be negative here. Therefore,  $\alpha_y, \alpha_z > 0$ .
- <sup>22</sup> For a review on the Landauer-Büttiker approach see: S. Datta, *Electronic transport in mesoscopic systems*, (Cambridge University Press, Cambridge, 1995).
- <sup>23</sup> The details of Feshbach projection for a similar problem using the same notation are given in Ref. 15.
- <sup>24</sup> A. Oguri, *J. Phys. Soc. Japan* **70**, 2666 (2001).
- <sup>25</sup> A reader not interested in how we compute the interacting Green's function entering the generalized Landauer-Büttiker formula might skip this subsection.
- <sup>26</sup> M. Salmhofer and C. Honerkamp, *Prog. Theor. Phys.* **105**, 1 (2001).
- <sup>27</sup> V. Meden, lecture notes on the

“Functional renormalization group”,

<http://www.theorie.physik.uni-goettingen.de/~meden/funRG/><sup>31</sup>

<sup>28</sup> For a review, see J. Sólyom, *Adv. Phys.* **28**, 201 (1979).

<sup>29</sup> We note that our approximate treatment of the two-particle interaction does not capture the Mott insulator state. As long as we stay away from half filling for long wires this is irrelevant in the present context.

<sup>30</sup> D. Grundler, *Phys. Rev. Lett.* **84**, 6074 (2000).

<sup>31</sup> Examples for the cutoff and spatial dependence of the renormalized parameters are given in J.E. Birkholz, PhD Thesis, Universität Göttingen (2008).

<sup>32</sup> K. Janzen, V. Meden, and K. Schönhammer, *Phys. Rev. B* **74**, 085301 (2006).